LAWRENCE
LIVERMORE
NATIONAL
LABORATORY

UCRL-PROC-202745

Polarization measurement of Iron L-shell lines on EBIT-I

H. Chen, P. Beiersdorfer, D. Robbins, A. J. Smith, M. F. Gu

March 7, 2004

The 4th International Plasma Polarization Symposium
Kyoto, Japan
February 3, 2004 through February 6, 2004

Polarization measurement of Iron L-shell lines on EBIT-I

Hui Chen, Peter Beiersdorfer
Lawrence Livermore National Laboratory, Livermore, CA 94551
Darron Robbins, A.J. Smith
Department of Physics, Morehouse College, Atlanta, GA 30314
Ming Feng Gu
Department of Physics, Stanford University, CA94305

Abstract

We report measurements of the line polarization of Ne-like and F-like of iron n=3 to n=2 transitions in the x-ray region. We used the "two-crystal technique" developed in previous polarization measurements in our laboratory. Preliminary results from our measurements are presented together with the theoretical calculations using the Flexible Atomic Code (FAC). Our calculations show that contributions from cascades play an important role in the polarization calculations of most of the transitions. The uncertainties and difficulties of our experiments are also discussed.

1. Introduction

Fe L-shell polarizations are important to laboratory studies relevant to astrophysics. Polarization processes have been demonstrated [1] to affect the emissions of many astrophysical sources. Another aspect of the relevance of polarization studies to astrophysics is based on the fact that polarizations can change the emission intensity, and therefore it has to be properly taken into account before one can extract other information from the emission. A good example is the Fe XVII line emission studies. Fe XVII lines have been observed in the Sun as well as in numerous cosmic sources studied with the Chandra and XMM-Newton observatories. Applications of these lines include using them as diagnostics for the source parameters. A laboratory measurement of the ratios of the 3s-2p to 3d-2p lines reported by Laming et al. [2] used the NIST electron beam ion trap and determined that the ratio 3s-2p and 3d-2p line intensities differed by nearly a factor of 2 from the same ratio measured from the Sun and Capella. Their results would have had far-reaching consequences for solar and astrophysics. However, another measurement from the Livermore EBIT group [3] strongly disagrees with the NIST measurements. The difference of the two measurements is as large as a factor of 2 at some data points. Careful calculations show good agreement with the later measurements. One of the many factors that resulted in the flawed results from the former measurement was later attributed to their neglect of polarization correction to the EBIT line emission.

In this report, we made use of the fact that the line emission from the EBIT source is polarized and measured the polarization of the Ne-like and F-like Fe lines that are of particular interests to astrophysics. This study is a part of the laboratory atomic database we are building. Related work includes the comprehensive Fe L-shell 3-2 line emission measurements that were completed a few years ago [4,5]. As will be shown in this report, these line measurements are the foundations of present measurements.

2. Experimental technique and instrumental setup

A number of previous polarization studies made on Livermore EBIT have established the "two crystal technique", which literally means that two crystal spectrometers are used for the experiment. The details of these techniques have been described elsewhere [6-8]. The equations for in this technique have been explained in detail by Beiersdorfer et al. [8]. The essence of this technique is summarized as the following.

For each line intensity dispersed by the crystal, we have $I_{meas.}=I_{//}R_{//} + I R$, R is the reflectivity of crystals. Line polarization is defined as $P = (I_{//} - I)/(I_{//} + I)$.

$$\left(\frac{I^a}{I^b}\right)_G = \frac{I^a_{//} + R_1 I^a}{I^b_{//} + R_1 I^b} = \frac{I^a_{//} + I^a}{I^b_{//} + I^b}, \qquad \left(\frac{I^a}{I^b}\right)_{Xtal} = \frac{I^a_{//} + R_2 I^a}{I^b_{//} + R_2 I^b} \tag{1}$$

If one has line b as a reference line, and the P_b is known, assuming $R= R / R_{//}$ is constant for the lines *a* and *b*, then we can derive the polarization for line *a* as:

$$P_a = \frac{\left(\frac{I^a}{I^b}\right)_G \left(1 + R_1 \frac{1-P_b}{1+P_b}\right)(R_2+1) - \left(\frac{I^a}{I^b}\right)_{Xtal} \left(1 + R_2 \frac{1-P_b}{1+P_b}\right)(R_1+1)}{\left(\frac{I^a}{I^b}\right)_G \left(1 + R_1 \frac{1-P_b}{1+P_b}\right)(R_2-1) - \left(\frac{I^a}{I^b}\right)_{Xtal} \left(1 + R_2 \frac{1-P_b}{1+P_b}\right)(R_1-1)} \tag{2}$$

Replacing one crystal spectrometer with a grating spectrometer, we have $R_{//} = R = 1$ for the grating measured intensity in Eq. (2).

The setup of the spectrometers on EBIT-I is shown in Fig 1. A flat field crystal spectrometer [9] was used. The crystal was RAP (2d=26.1Å). The grating spectrometer uses a 44.3m grazing-incidence grating which has variable line spacing of about 2400 l/mm. It features with high resolving power and larger wavelength coverage (10 - 50 Å). It used a liquid nitrogen cooled back- illuminated CCD as detector.

Our data was all taken in steady state. The electron beam energies were set so that we can maximize the population of the desired charge states. This is illustrated in Fig.2. At the beam energy of 1.3 keV, the Ne-like Fe ions are dominant, as shown by the strong Ne-like lines, compared to the spectrum at 1.4 keV where the F-like lines are very strong. At 1.5 keV, Ne-like lines have almost vanished while F-like and O-like lines take the stage. In addition to the feature of "charge state selectiveness", by applying different beam energy, one can actually "select" emission processes, such as minimizing emission from resonance excitations or dielectronic recombinations. These two "selective" features made EBIT an ideal device to quantitatively measure atomic data including the line polarization.

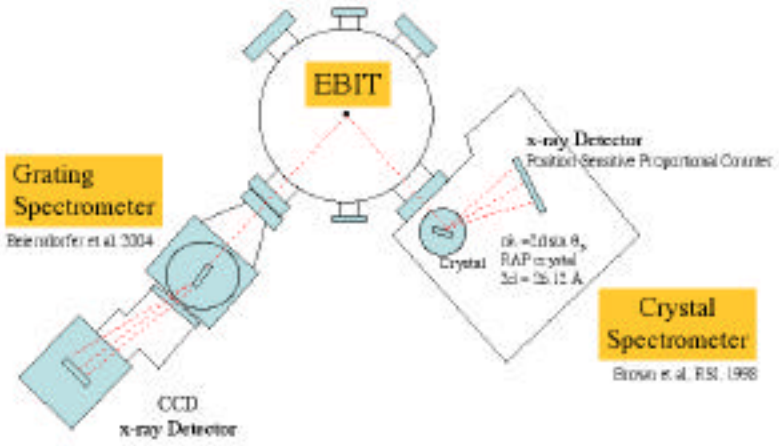

Figure 1: Diagram of the experimental setup.

In our experiment, the Ne-like Fe spectral data were taken at beam energies at 850 to 1400 eV. The F-like Fe data were taken at 1300 to1500 eV. The grating spectrometer covered the interested spectral range of 13-18Å, while we needed two crystal settings to cover the same wavelength interval.

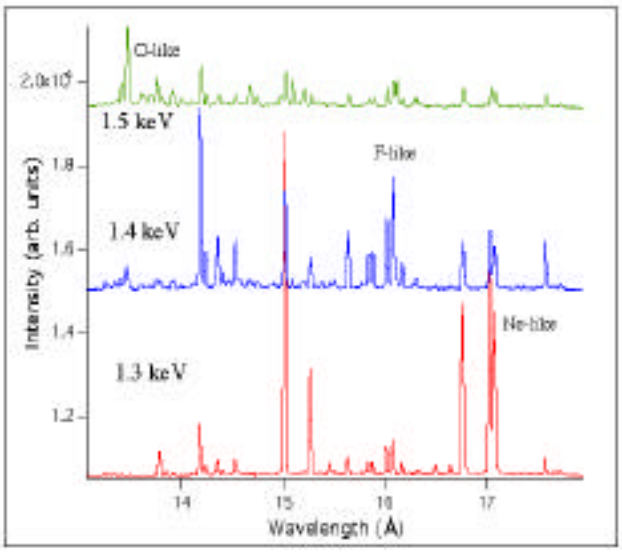

Figure 2. Fe spectra at three electron beam energies.

3. Experimental results and discussion

3.1.Ne-like Fe

We have obtained Ne-like Fe spectra at 800 to 1300 eV beam energies in the region covering the six well known n=3 to n=2 transition lines:

3C $1s^2 2s^2 2s2p2p^4 3d_{3/2} \rightarrow 1s^2 2s^2 2p^6$ **3D** $1s^2 2s^2 2p^2 2p^3 3d_{5/2} \rightarrow 1s^2 2s^2 2p^6$
3E $1s^2 2s^2 2p^2 2p^3 3d_{3/2} \rightarrow 1s^2 2s^2 2p^6$ **3F** $1s^2 2s^2 2p2p^4 3s_{1/2} \rightarrow 1s^2 2s^2 2p^6$
3G $1s^2 2s^2 2p^2 2p^3 3s_{1/2} \rightarrow 1s^2 2s^2 2p^6$ **M2** $1s^2 2s^2 2p^2 2p^3 3s_{1/2} \rightarrow 1s^2 2s^2 2p^6$

We determined the grating spectrometer response using the H-like Oxygen lines. As showing in Fig. 3, the H-like Oxygen lines have good spectral overlap with the Ne-like Fe lines.

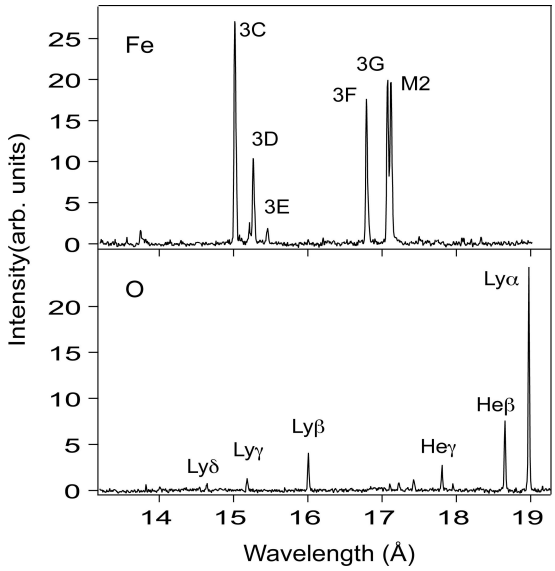

Fig. 3. Fe and O spectra taken with the grating spectrometer

Using the theoretical Lyβ/Lyα ratio as standard, the spectrometer response is determined by the deviation of the measured Lyβ/Lyα ratio from the theoretical calculations. Figure 4. shows the results of measurements and two types of theoretical calculations, one is from APEC [10] and one is from the FAC code [11]. Weighted measurements (thin blue line) and weighted error (grey area) overlay well with the FAC calculations. This indicates a constant response of the grating spectrometer for the wavelength range we are interested in.

The efficiency of the crystal spectrometer was determined by taking into account the window foils and the absorption of the detector. The result is given in Fig. 5. These response functions were then folded in the measured line intensities during analysis.

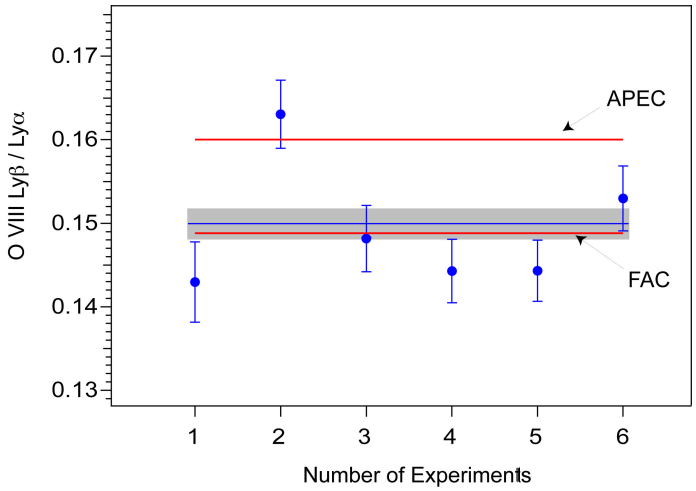

Figure 4. OVIII Lyβ/Lyα ratios from the grating spectrometer measurements (dots with error bars) and model calculations (red lines each from FAC and APEC).

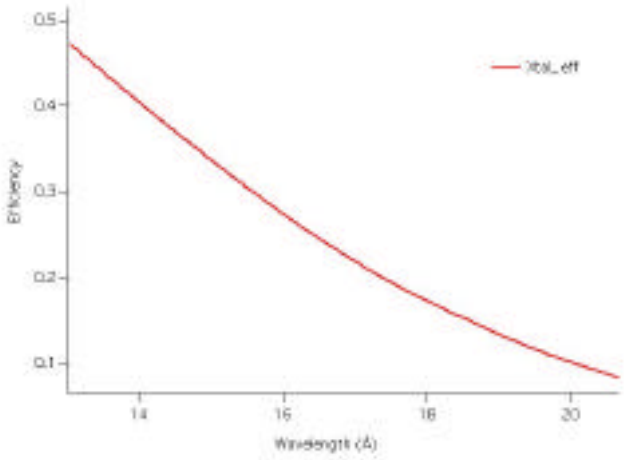

Figure 5. The efficiency of the crystal spectrometer in the wavelength range of interest.

We used the 3C line as reference/normalization P_{3C}=0.4. Figure 6 shows the overlap of two spectra taken with the grating and crystal spectrometers. It is from the difference of the line ratios of the two spectrometers that the polarization was determined, as described by equation (1) and (2).

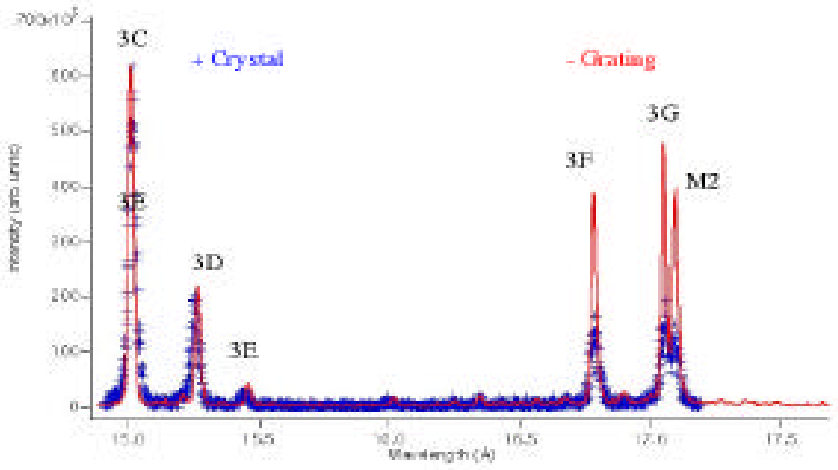

Figure 6. Ne-like Fe spectra from the grating spectrometer and from the crystal spectrometer.

The derived polarization of the 3D line is shown in Fig 7. Using the FAC code, we calculated the theoretical polarization under two conditions. One takes into account of the contribution of radiative cascades, the other does not. For 3D line, the prediction from the two cases differs slightly, as showing in the Fig. 7. For other Ne-like lines, the two calculations give a very different answer. Overall, the calculations taking the cascades into account give more realistic answer and compare better with experiments.
The Polarizations for 3E, 3F, 3G and M2 lines are also derived. The results are listed in Table 1 – 4. The error bar on the experimental data is not yet in its final form, but we expect it to be as large as 30-60%.

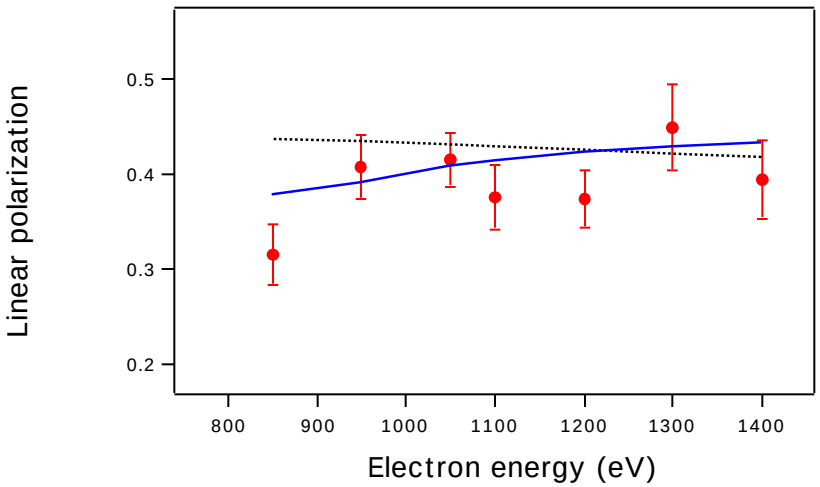

Figure 7. Comparison of the polarization of 3D from measurements (dots with error bars) and FAC calculations with the contributions from cascades taken into account (solid line) and not taken into account (dotted line).

Table 1: Polarization measurement and calculations for 3E line.

Energy (eV)	Polarization	FAC (cascades)	FAC (no cascades)
850	-0.37	-0.39	-0.19
950	-0.20	-0.34	-0.17
1050	-0.40	-0.33	-0.14
1100	-0.21	-0.32	-0.13
1200	-0.39	-0.29	-0.10

Table 2: Polarization measurement and calculations for 3F line.

Energy (eV)	Polarization	FAC (cascades)	FAC (no cascades)
850	-0.10(0.03)	0.067	0.57
950	-0.13(0.04)	0.068	0.56
1050	-0.17(0.03)	0.071	0.56
1100	-0.10(0.04)	0.072	0.56
1200	-0.12(0.03)	0.074	0.55
1300	-0.24(0.05)	0.076	0.55
1400	-0.34(0.05)	0.078	0.54

Table 3: Polarization measurement and calculations for 3G line.

Energy (eV)	Polarization	FAC (cascades)	FAC (no cascades)
850	-0.22	0.052	0.58
950	-0.18	0.051	0.57
1050	-0.22	0.056	0.57
1100	-0.19	0.058	0.56
1200	-0.27	0.061	0.56
1300	-0.30	0.065	0.55

Table 4: Polarization measurement and calculations for M2 line.

Energy (eV)	Polarization	FAC (cascades)	FAC (no cascades)
850	-0.23	-0.10	-0.24
950	-0.22	-0.13	-0.24
1050	-0.22	-0.12	-0.23
1100	-0.25	-0.12	-0.23
1200	-0.21	-0.12	-0.23
1300	-0.31	-0.11	-0.22

3.2 F-like Fe lines

F-like 3-2 Fe spectra are much more complicated. They contain many more lines in the wavelength region of 14 Å – 18 Å. Fig.8 shows three F-like Fe spectra taken with the grating and crystal spectrometers at the electron energy of 1.35 keV. The F-like Fe lines have all been identified previously [5]. The lines and their corresponding transitions are listed in Table 5.

Applying the same technique as described earlier, we have some preliminary line polarization results for some of the strong lines. Since this analysis is not yet complete, we cannot draw concrete conclusions. So far we found that the polarization analysis is very sensitive to the variation of the line intensities, and small errors in the line intensity fitting could result in amplified error in the polarization values. Also, the derived polarization appeared to be quite different if we use lines from different charge states as normalization. As an illustration, Fig. 8 shows our preliminary results for line F11. Several other F-like Fe lines seem to have a similar pattern as F11. This could due to some artifacts of our analysis, or could be caused by some new physics that is unknown to us. We are going to further investigate this issue, for which both further analysis and new experiments will be needed.

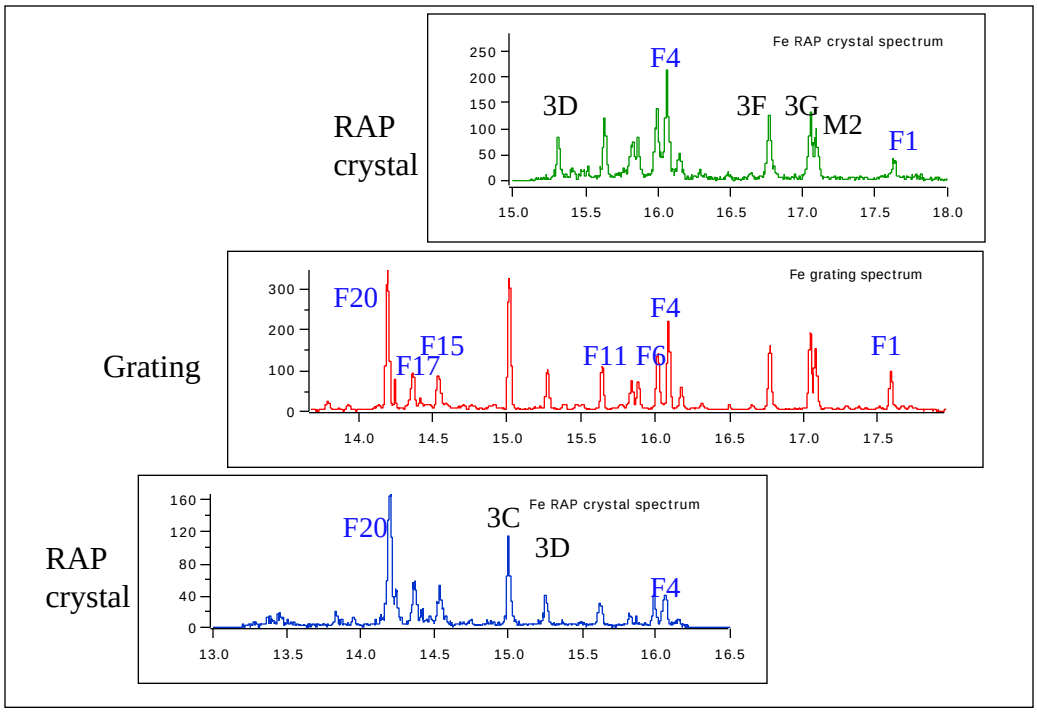

Figure 8. Fe spectra at the electron beam energy of 1.35 keV. Strong lines are marked and the labels of the F-like lines use the line labels of Brown et al.

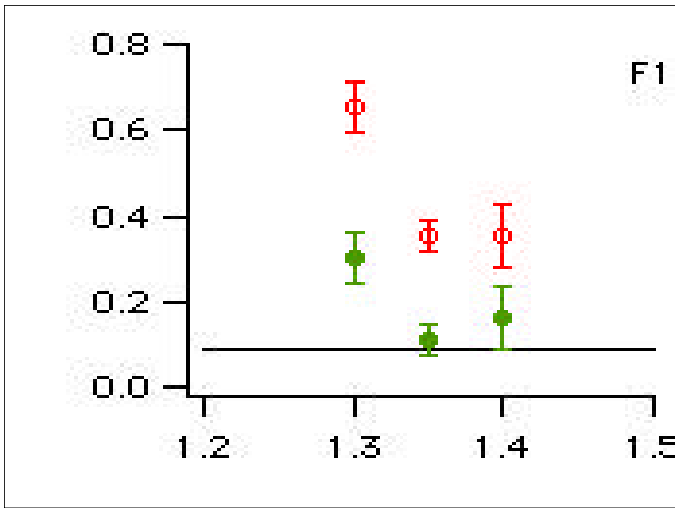

Figure 9. Polarization of the F1 line from analysis using line 3G as normalization (circles with error bar) and using line F4 as normalization (dots with error bar). The FAC calculation is shown in solid line.

In conclusion, using the “two-crystal technique”, we measured the polarization of Ne-like and F-like Fe lines using the Livermore EBIT. We have achieved good Ne-like Fe measurements. The F-like Fe analysis did not yet give a consistent picture; we hope further experiments will be performed to shine more light on these puzzling results.

Table 5: F-like Fe line indentifications

LABEL	Upper	J'	Lower	J	λ (Å)
F1[d]	$1s^2 2s^2 2p_{1/2} 2p_{3/2}^3 3p_{1/2}$	$\frac{3}{2}$	$1s^2 2s_{1/2} 2p^2 2p^4$	$\frac{1}{2}$	17.664
F2	$1s^2 2s_{1/2} 2p^2 2p_{3/2}^3 3s$	$\frac{3}{2}$	$1s^2 2s_{1/2} 2p^2 2p^4$	$\frac{1}{2}$	16.345
F3	$1s^2 2s_{1/2} 2p_{1/2} 2p^4 3s$	$\frac{3}{2}$	$1s^2 2s_{1/2} 2p^2 2p^4$	$\frac{1}{2}$	16.197
F4	$1s^2 2s^2 2p^2 2p_{3/2}^2 3s$	$\frac{5}{2}$	$1s^2 2s^2 2p^2 2p_{3/2}^3$	$\frac{3}{2}$	16.097
F5	$1s^2 2s^2 2p_{1/2} 2p_{3/2}^3 3s$	$\frac{1}{2}$	$1s^2 2s^2 2p_{1/2} 2p^4$	$\frac{1}{2}$	16.044
F6	$1s^2 2s^2 2p^2 2p_{3/2}^2 3s$	$\frac{3}{2}$	$1s^2 2s^2 2p^2 2p_{3/2}^3$	$\frac{3}{2}$	16.023
F7	$1s^2 2s^2 2p^2 2p_{3/2}^2 3s$	$\frac{1}{2}$	$1s^2 2s^2 2p^2 2p_{3/2}^3$	$\frac{3}{2}$	15.901
F8	$1s^2 2s^2 2p_{1/2} 2p_{3/2}^3 3s$	$\frac{3}{2}$	$1s^2 2s^2 2p_{1/2} 2p^4$	$\frac{1}{2}$	15.883
F9	$1s^2 2s^2 2p_{1/2} 2p_{3/2}^3 3s$	$\frac{3}{2}$	$1s^2 2s^2 2p^2 2p_{3/2}^3$	$\frac{3}{2}$	15.853
F10	$1s^2 2s^2 2p_{1/2} 2p_{3/2}^3 3s$	$\frac{1}{2}$	$1s^2 2s^2 2p^2 2p_{3/2}^3$	$\frac{3}{2}$	15.787
F11	$1s^2 2s^2 2p_{1/2} 2p_{3/2}^3 3s$	$\frac{5}{2}$	$1s^2 2s^2 2p^2 2p_{3/2}^3$	$\frac{3}{2}$	15.641
F12	$1s^2 2s_{1/2} 2p^2 2p_{3/2}^3 3s$	$\frac{3}{2}$	$1s^2 2s_{1/2} 2p^2 2p^4$	$\frac{1}{2}$	15.501
F13	$1s^2 2s^2 2p^2 2p_{3/2}^2 3d_{5/2}$	$\frac{1}{2}$	$1s^2 2s^2 2p^2 2p_{3/2}^3$	$\frac{3}{2}$	14.601
F14	$1s^2 2s^2 2p^2 2p_{3/2}^2 3d_{5/2}$	$\frac{3}{2}$	$1s^2 2s^2 2p^2 2p_{3/2}^3$	$\frac{3}{2}$	14.568
F15	$1s^2 2s^2 2p^2 2p_{3/2}^2 3d_{5/2}$	$\frac{5}{2}$	$1s^2 2s^2 2p^2 2p_{3/2}^3$	$\frac{3}{2}$	14.548
F16	$1s^2 2s^2 2p_{1/2} 2p_{3/2}^3 3d_{5/2}$	$\frac{3}{2}$	$1s^2 2s^2 2p_{1/2} 2p^4$	$\frac{1}{2}$	14.424
F17	$1s^2 2s^2 2p_{1/2} 2p_{3/2}^3 3d_{3/2}$	$\frac{5}{2}$	$1s^2 2s^2 2p^2 2p_{3/2}^3$	$\frac{3}{2}$	14.386
F18	$1s^2 2s^2 2p_{1/2} 2p_{3/2}^3 3d_{3/2}$	$\frac{1}{2}$	$1s^2 2s^2 2p_{1/2} 2p^4$	$\frac{1}{2}$	14.360
F19	$1s^2 2s^2 2p_{1/2} 2p_{3/2}^3 3d_{3/2}$	$\frac{1}{2}$	$1s^2 2s^2 2p^2 2p_{3/2}^3$	$\frac{3}{2}$	14.276
	$1s^2 2s^2 2p_{1/2} 2p_{3/2}^3 3d_{5/2}$	$\frac{5}{2}$	$1s^2 2s^2 2p^2 2p_{3/2}^3$	$\frac{3}{2}$	14.267
F20	$1s^2 2s^2 2p_{1/2} 2p_{3/2}^3 3d_{5/2}$	$\frac{3}{2}$	$1s^2 2s^2 2p^2 2p_{3/2}^3$	$\frac{3}{2}$	14.216
	$1s^2 2s^2 2p_{1/2} 2p_{3/2}^3 3d_{3/2}$	$\frac{5}{2}$	$1s^2 2s^2 2p^2 2p_{3/2}^3$	$\frac{3}{2}$	14.203

By Brown et al., Apj supp. 140, 589 (2002)

Reference

[1] Csanak, G., Review talk at this conference, (2004)
[2] Laming, J. M, et al, ApJ., 545, L161, (2000)
[3] Beiersdorfer, P. et al, ApJ, 576, L169, (2002)
[4] Brown, G, V., et al Apj, 502 1015 (1998)
[5] Brown, G.V, et al, ApJ. Sup. 140, 589, (2002)
[6] Wargelin, B. J., PhD thesis, University of California, Berkeley, (1993), UCRL-LR-115961
[7] Beiersdorfer et al. PRA, 53, 3974,(1996)
[8] Beiersdorfer, P., et al, PRA 60, 4156 (1999)
[9] Brown et at. RSI, 70, 280 (1999)
[10] APEC: Astrophysical plasma emission code
[11] Gu, M. F., ApJ, 582, 1241, 2003

This work was performed under the auspices of the U.S. Department of Energy by the University of California, Lawrence Livermore National Laboratory under Contract W-7405-Eng-48.